PROCEEDINGS OF SCIENCE

Comprehensive estimate of the sensitivity of ANITA to tau neutrinos

Stephanie Wissel*
California Polytechnic State University, San Luis Obispo, CA USA
E-mail: swissel@calpoly.edu

Claire Burch[1,2], Washington Carvalho Jr.[3,4], Joe Crowley[5], Jaime Alvarez-Muñiz[6], Austin Cummings[7], Abdulrahman Kauther[5], Andrés Romero-Wolf[1,3], Harm Schoorlemmer[8], Enrique Zas[6]

[1]*Jet Propulsion Laboratory, Pasedena, CA USA;* [2]*Harvard College, Harvard University, Cambridge, MA USA;* [3]*California Institute of Technology, Pasedena, CA USA;* [4]*Departamento de Fśica, Universidade de São Paulo, São Paulo, Brazil;* [5]*California Polytechnic State University, San Luis Obispo, CA USA;* [6] *Departamento de Física de Partículas & Instituto Galego de Física de Altas Enerxías, Univ. de Santiago de Compostela, Spain;* [7]*Gran Sasso Science Institute, School of Advanced Studies, L'Aquila, Italy;* [8]*Max-Planck-Institut für Kernphysik, Heidelberg, Germany*

and the ANITA Collaboration†

Two anomalous events have been reported by the ANITA collaboration that are observationally consistent with air showers from a particle emerging from the Antarctic ice. One possible interpretation of these events is that they are due to tau neutrinos interacting in the Earth, resulting in an air shower initiated by a tau lepton decay. We present a comprehensive study of the sensitivity of ANITA to tau neutrinos, using the expected Standard Model cross-sections and tau lepton energy losses, varied ice thicknesses, and radio emission simulation of upgoing tau showers with ZHAireS.

36th International Cosmic Ray Conference -ICRC2019-
July 24th - August 1st, 2019
Madison, WI, U.S.A.

*Speaker.
†for collaboration list, see PoS(ICRC2019)1177 or https://anitaneutrino.github.io/authorlist

PoS(ICRC2019)1034

1. Introduction

ANITA is a NASA long-duration balloon payload designed to detect the highest energy cosmic neutrinos via the radio technique. Neutrinos generate radio emission via the Askaryan radiation, which is impulsive, coherent radio Cherenkov emission emitted by particle cascades in dense dielectric materials like ice. ANITA takes advantage of the long attenuation lengths of ice and its high flight altitude (35-40 km) to monitor a large volume of ice.

ANITA also observes coherent radiation from air showers. Air showers generate radio emission dominated by the geomagnetic effect due to time-varying currents generated as an air shower develops in the Earth's magnetic field. Most cosmic rays in ANITA are observed as reflected events where the electric fields generated by the downgoing showers have inverted in polarity relative to the direct, unreflected cosmic rays.

Two anomalous air shower events were observed in the first and third ANITA flights [1, 2]. Both events were impulsive and their polarization angle correlated with the expectation from the Earth's geomagnetic field, as expected for a typical air shower event. However, both also have polarity consistent with direct cosmic rays, but arrive from steeply upgoing angles of -27.4° and -35° with respect to the horizon.

We considered in Ref. [3] the hypothesis that these two events are due to an isotropic flux of tau neutrinos. We concluded that both the steepness of the events and the limits from the standard search with ANITA, IceCube, and Auger exclude this possibility based on a comprehensive estimate of the upper bound on the ANITA exposure to the air shower tau channel. In this proceeding, we summarize the analysis of the tau neutrino air shower channel and update it to include the ANITA-IV flight. We conclude by making an order of magnitude estimate of the sensitivity of ANITA to a point source of tau neutrinos via the air shower channel.

2. Monte Carlo of ANITA Exposure to an Isotropic Tau Flux

In this section, we describe our model for the ANITA acceptance and exposure to an isotropic flux of tau neutrinos via the air shower channel. Several optimistic assumptions are made in an effort to estimate the maximum possible exposure of ANITA to tau neutrinos.

As shown in Fig. 1, an upgoing tau neutrino may be observed at the ANITA payload after undergoing a charged current interaction in the Earth to produce a tau lepton that decays in air. Both the neutrino and tau lepton propagate along a direction defined by $\hat{r}_{\nu_\tau}$. The tau exits at a point defined by the Earth angle θ_E and zenith angle local to the exit point θ_{exit} and decays at an altitude above the ice surface of thickness D. Several decay products of the tau lepton can result in extensive air showers, specifically the hadrons, electrons, and gammas. The extensive air showers produce impulsive, radio frequency radiation that can be observed at the ANITA payload at an altitude above sea level h and at an angle from the decay point, $\theta_{\rm view}$.

In the Monte Carlo, both charged current and neutral current interactions of tau neutrinos in the Earth are tracked in terms of their energy loss and probability that a tau lepton will exit, P_{exit}, through NuTauSim [4]. We allow for a range the cross sections that fall within the uncertainties allowed by the Standard Model [5] and two models for energy loss of the tau lepton [6, 7]. The tau decay point is exponentially sampled within a decay length of $L_{decay} = 49$ km (E_τ/EeV). Events

that decay beyond the detector do not contribute to the acceptance, which is particularly important at high energies. We model the radio emission from the tau decay using a modified version of the ZHAireS that produces radio emission from upward-going tau lepton decays.

The most common decay mode injects 98% of the tau lepton energy into pions ($\pi^0\pi^-\nu_\tau$) and we use this decay mode modeled with TAUOLA [8] for the ZHAireS simulations. In the previous analysis [3], we assumed that all the tau energy was deposited into the shower, but in this analysis we refine this calculation to account for energy that goes into non-showering particles. The fraction of energy transferred from the tau lepton to the shower is estimated by sampling a distribution of Pythia [9] simulated decays. The energy fraction distributions have a mean of 0.56 and a 68% confidence interval of ranging from 0.25 to 0.87.

Showers were simulated with a magnetic field of 60 μT for a range of zenith angles and decay altitudes. The magnetic field is oriented perpendicular to the direction of the shower to maximize the electric field strength in this upper limit calculation. The electric field is filtered in the 180-1200 MHz band to match the trigger band of ANITA-III. For ANITA-IV, the magnitude of the loss due to the programmable notch filters called the TUFFs (see Sec. 3) are modeled as Gaussians in the frequency domain, as shown in the blue curve in Fig. 2. A ring-like radio emission pattern forms evident in the lateral distribution functions shown on the right in Fig. 2. The peak of the lateral distribution function does not uniformly increase with decreasing distance, but rather the decrease in the density of the atmosphere and the decrease of the distance from the shower to the observer with increasing decay altitude causes the showers to become more extended and not fully developed before reaching the detector. An additional loss of coherence due to variations in the view angle between the shower and the detector further contributes to the decrease of the peak electric field at higher altitudes.

Following the description in Ref. [3], the radio emission beam patterns are parameterized as a function of zenith angle at the decay point and decay altitude above the ice. The fits are represented by the combination of a Gaussian and Lorentzian centered on the peak $\theta_{\rm view}$ along with a Gaussian centered at $\theta_{\rm view} = 0^\circ$. The shape is given by

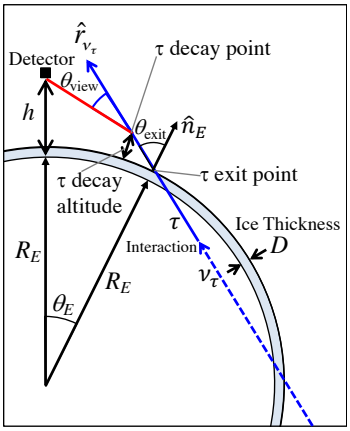

Figure 1: Detection geometry from Ref. [3]. An incoming neutrino (blue dashed line) impacts a spherical Earth with polar radius R_E that has an additional layer of ice of thickness D above it. If the neutrino undergoes a charged current interaction, a tau lepton is produced that propagates along the same direction, $\hat{r}_{\nu_\tau}$ as the neutrino. The tau may then exit the Earth's surface at an exit point defined by the Earth angle θ_E and the exit angle $\theta_{\rm exit}$. The tau lepton then decays at a point above the ice surface and may produce an extensive air shower. The air shower generates radio emission that is viewed by ANITA flying at altitude h above R_E at an angle $\theta_{\rm view}$ from the decay point.

$$\varepsilon(\theta_{\rm view}) = E_0\left[f\exp\left(-\frac{(\theta_{\rm view}-\theta_{\rm pk})^2}{2\sigma_{\rm view}^2}\right) + (1-f)\left(1+\left(\frac{\theta_{\rm view}-\theta_{\rm pk}}{\sigma_{\rm view}}\right)^2\right)^{-1}\right] + E_1\exp\left(-\frac{\theta_{\rm view}^2}{2\Sigma_{\rm view}^2}\right) \tag{2.1}$$

and the electric field is

$$E_{\text{peak}}(\mathscr{E}_\tau, r, \theta_{\text{view}}) = \left(\frac{\mathscr{E}_\tau}{10^{17}\text{ eV}}\right)\left(\frac{r}{r_0}\right)^{-1}\varepsilon(\theta_{\text{view}}). \tag{2.2}$$

where r_0 is the distance from ANITA to the τ lepton decay point. Fig. 2(right) shows the parameterization for the 180-1200 MHz band that includes the model of the TUFF response. We use a simplified model of the ANITA trigger that assumes an electric field threshold and approximates a voltage threshold at a single frequency (300 MHz). If the electric field of a simulated tau event is above this threshold at the payload, it results in a trigger.

The final numerical estimate of the acceptances multiplies the maximal aperture by the summed probabilities of events thrown in the Monte Carlo. The maximal aperture is estimated semi-analytically in Motloch *et. al* to be $A_0 = 2\pi^2 R_E h/(1+h/R_E)$.

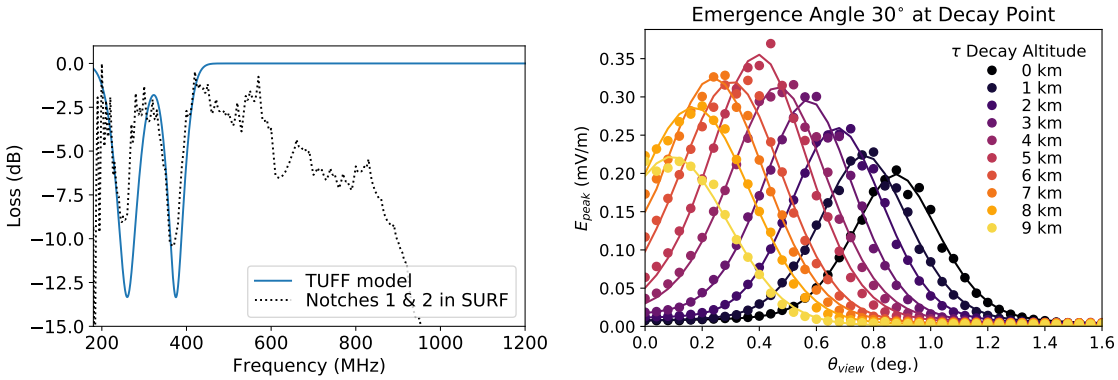

Figure 2: (left) The loss induced by applying the two programmable notch filters (the TUFFs) in ANITA-IV. The loss model (blue solid line) at the trigger level assumed in the Monte Carlo compared to the loss measured in the digitizer signal chain (black dotted line), which has loss at high frequencies not present at the trigger level. The peak electric field vs. θ_{view} from ZHAireS simulations of a 10^{17} eV τ lepton decay at emergence angle 30° and for decay altitudes from 0 km to 9 km (dots) compared with the parameterized fits (lines).

3. ANITA Electric Field Thresholds

There have been four flights of the ANITA experiment. With each flight, the experiment has lowered its electric field threshold to cosmic rays by either lowering the voltage signal-to-noise ratio (*SNR*) at which the trigger reaches its 50% point or the system temperature, T_{sys}, as shown in Tab. 1. Additionally, the bandwidth of the antennas used on ANITA-III and IV was expanded to 180-1200 MHz from the earlier ANITA-I and II bandwidth of 200-1200 MHz.

For each flight, the electric field thresholds are assumed to be scaled based on the weakest cosmic ray event observed in ANITA-I (A_1 in Eqn. 3.1). The electric field threshold for the i-th ANITA flight is given by:

$$E_{th} = E_{th,A_1}\frac{SNR_{A_i}}{SNR_{A_1}}\sqrt{\frac{T_{sys,i}}{T_{sys,A_1}}} \tag{3.1}$$

ANITA Flight	I	III	IV
Livetime (days)	17.4	17.4	24.25
SNR at 50% Trigger Efficiency	5.4	3.9	3.7
System temperature (K)	245	295	160
Electric Field Threshold (mV/m)	446	287	234

Table 1: Livetimes and electric field thresholds for air showers assumed in the Monte Carlo and flight times as described in text. The ANITA-II trigger was biased against horizontally polarized triggers, and is therefore, not included here.

During the ANITA-III flight, continuous wave (CW) radio-frequency interference (RFI) from satellites from the North significantly impacted the exposure of the instrument, because the regions of the payload pointed towards the north were masked from the trigger (an effect called phi-masking) such that the masked fraction of the payload was always below 30%. Masking impacts the total exposure of the ANITA-III instrument, but not the acceptance.

During ANITA-IV, programmable notch filters called TUFFs, allowed the instrument to achieve a factor of 2.8 higher livetime than ANITA-3. Two notches were enabled for the entire duration of the ANITA-IV flight. Notch 1 had a center frequency of 260 MHz; Notch 2, 375 MHz. The average loss shown in Fig. 2 (left) due to the TUFFs was measured on the SURF-v3 digitizers, which have significant loss at higher frequencies that is not present in the trigger signal chain. We additionally assume that the 10% reduced bandwidth from the two notches used on ANITA-4 lowered the electric field threshold by $\sqrt{90\%}$. Because the signal received at the trigger is lower, the loss at lower frequencies affects the overall acceptance of ANITA-IV.

4. ANITA Acceptance and Exposure to an Isotropic Tau Flux

Fig. 3 (left) compares the upper bound on the acceptance of ANITA's air shower channel to an isotropic tau neutrino flux to the acceptances of IceCube [10] and Auger to the Earth-skimming ν_τ channel [11]. The ANITA air shower channel has a comparable acceptance to IceCube and Auger within a factor of 2 at energies above 3×10^{18} eV. While the acceptance to the air shower channel plateaus above this energy because an increasingly larger fraction of taus decay at higher altitudes or beyond the detector, the acceptance of ANITA to tau neutrinos via the Askaryan channel grows with energy. However, because the air showers are in general closer to the detector than the in-ice showers, the air shower channel has a lower energy threshold.

The lower trigger threshold and wider bandwidth of ANITA-III resulted in a higher overall acceptance for ANITA-III than ANITA-I. Even though ANITA-IV has a lower trigger threshold than the previous flights, the acceptance achieved by ANITA-IV is a factor of two lower than ANITA-III. This is because the two TUFF notches were in the lower portion of the frequency band and the radio signal is low-frequency dominant.

The total upper bound to the summed exposure of the three ANITA flights is shown on the right in Fig. 3. The blue band brackets variations on the energy loss model of tau leptons propagating in the Earth, the thickness of the ice, and the ranges of Standard Model cross-sections. Even though the acceptances are comparable, ANITA's air shower channel has a substantially smaller exposure

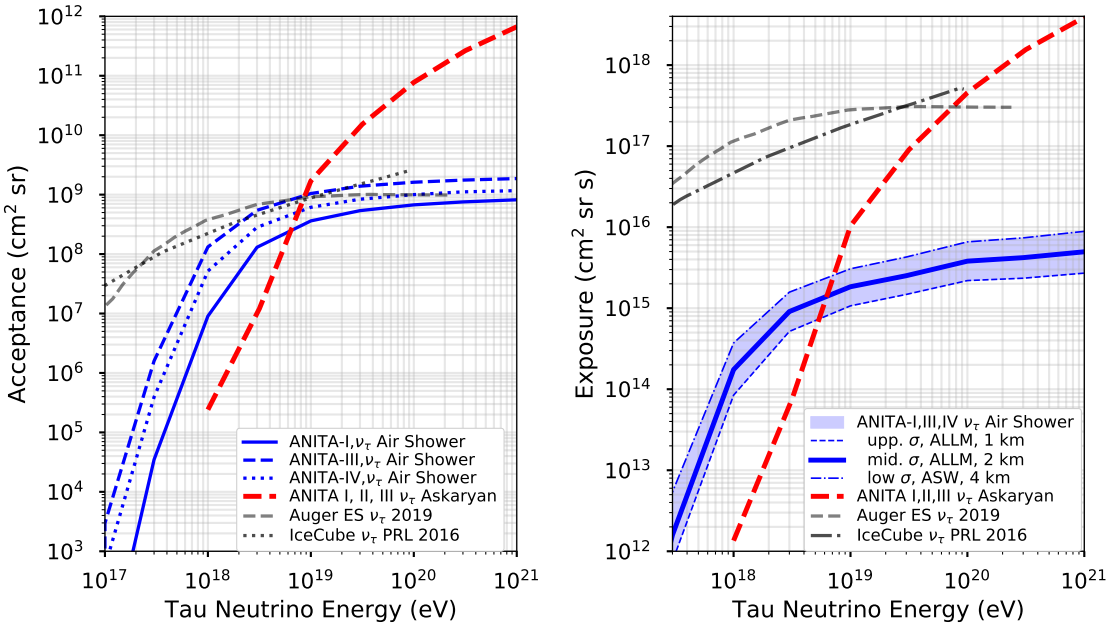

Figure 3: Upper bound estimates of the ANITA acceptance (left) and summed exposure (right) to tau neutrinos (blue lines and band) compared to the Earth skimming (ES) ν_τ channel of Auger (dashed grey lines) [11], IceCube ν_τ (dot-dashed darker grey line) [10], and the ANITA Askaryan search for in-ice showers from ν_τ's (red dashed line) [12]. (left) The acceptance of ANITA-I,III, and IV to τ-lepton air showers (blue lines) assuming mean values of cross section, an ALLM [6] energy loss model and 2.0 km ice thickness. (right) The blue-shaded band includes the range of variations due to assumptions on the ice thickness (1-4 km), neutrino cross section, and τ energy loss models. The minimum exposure (dashed blue line) assumes a high cross section, the ALLM [6] energy loss model, and 1 km ice thickness, while the maximum exposure (dot-dashed blue) assumes a low cross section, the ASW [7] energy loss model, and 4 km ice thickness. The solid blue line assumes a mean value for the cross section, ALLM energy loss model, and ice thickness of 2 km.

than IceCube, Auger, and the ANITA Askaryan channel. Variations in the cross section, energy loss model, and ice thickness contribute to at most a factor of 3 change in the total exposure.

5. Point Source Sensitivity

While the exposure of ANITA to an isotropic tau neutrino flux via the air shower channel is significantly suppressed compared to other long running experiments, ANITA has a deep effective area in the direction of the horizon. We report in this section preliminary bounds on ANITA's point source sensitivity both in the directions of the anomalous events and towards the horizon where the effective area is the deepest. This estimate is accurate only to within an order of magnitude for showers of energy 0.6 EeV and will be updated with the refinements applied to the isotropic tau flux.

The effective area can be estimated by calculating the maximum geometric effective area for a radio receiver at a given detector altitude and multiplying that by the combined probabilities that a tau lepton will exit the Earth, that it will decay and that the shower will be detected. We evaluated the maximum geometric effective area for a neutrino coming from a point source in a

Flight	$\langle A \rangle_g$	Emergence Angle	P_{exit}	$P_{E,shower}$	$\langle A \rangle_{eff}$
ANITA-I	5.54 km^2	26.8°	8×10^{-6}	$\leq 5 \times 10^{-2}$	$\leq 2.2\ m^2$
ANITA-III	5.75 km^2	34.5°	1×10^{-6}	$\leq 5 \times 10^{-2}$	$\leq 0.3\ m^2$

Table 2: Upper bound on the effective area of ANITA to a point source of tau neutrinos.

E_{shower}	P_{exit}	$P_{E,shower}$	$\langle A \rangle_{peak}$
10^{18} eV	2.5×10^{-3}	0.5	1.9×10^5 m^2
10^{19} eV	3.5×10^{-3}	0.5	2.6×10^5 m^2

Table 3: Upper bound on the effective area of ANITA to a point source at an emergence angle of 3.9°

given direction $\hat{r}_*$ (equivalent to r_{ν_τ} in Fig. 1) with a Monte Carlo as:

$$\langle A \rangle(\hat{r}_\nu) = A_0 \sum_{i=0}^{N} \hat{n}_E \cdot \hat{r}_* \Theta(\theta_{cut} - \theta_{view}), \tag{5.1}$$

where the normal vector at the exit point, $\hat{n}_E$, and view angle, θ_{view} are as illustrated in Fig. 1. The heaviside step function, $\Theta(\theta_{cut} - \theta_{view})$ requires that only events observed within a certain view angle are detectable. We assume an altitude of 35.5 km and an ice thickness of 4.0 km. We assume that all events within the radio beam pattern of a view angle of $\theta_{cut} = 1^\circ$ trigger the instrument, consistent with the beam patterns shown in Fig. 2 (right). All of the events decay before reaching the detector, since ANITA is more than 60 km away from the exit point, and we assume that all the taus decay immediately upon exiting the Earth's crust.

We can first estimate the effective area at the angles associated with the anomalous events, using the calculations of the exit probabilities and exiting tau energies calculated by Alvarez-Muñiz *et. al* [4]. The probability that a tau will exit converges to the values shown in the table for all initial tau neutrino energies for angles above 20° [4]. The observed shower energies of 0.6 EeV lie outside the 95% confidence interval of distributions of the energies of the tau lepton at the steep angles of the two anomalous events. Thus we assume the probability that a tau shower results from a tau neutrino interaction to be less than 5×10^{-2}. The resulting effective area is at most 2.2 m^2 for ANITA-I and 0.3 m^2 for ANITA-III, as summarized in Tab. 2. Given that the total livetime of IceCube is substantially longer than three flights of ANITA, we conclude that ANITA's sensitivity to repetitive transient sources at the observed shower energies and steep angles of the anomalous events is substantially lower than IceCube's sensitivity [13].

We can additionally consider the sensitivity of ANITA near the horizon, where ANITA achieves its peak geometric effective area of 150 km^2 at an emergence angle of 3.9°. The electric field thresholds assumed for ANITA-I and III in Tab. 1 translate to threshold shower energies of $10^{17.9}$ eV and $10^{17.4}$ eV. Based on inspection of the tau lepton energy distributions, the threshold shower energies are ∼50% likely to result from a tau neutrino interaction [4]. We estimate that the upper bound on the effective area of ANITA is $\mathcal{O}(10^5)$ m^2 in the two energies shown in Tab. 3, which is comparable to the peak effective area of Auger [14].

6. Discussion

We presented an updated estimate to ANITA's acceptance and exposure to an isotropic tau neutrino flux that includes ANITA-IV. The estimate is an upper bound based on a comprehensive Monte Carlo that models the tau neutrino interaction, tau decay and radio emission, and ANITA trigger. Given that other experiments, including the ANITA Askaryan search, achieve exposures that are factors of 40 to several orders of magnitude higher than what is achieved with the tau channel, we find that an isotropic tau neutrino flux is disfavored.

Additionally, we make an order-of-magnitude estimate of ANITA's sensitivity to point sources and find that while the effective area at the steeply inclined angles observed in the ANITA anomalous events is on the few m^2sr scale, ANITA's sensitivity to transient point sources at the horizon is comparatively deeper.

Acknowledgements ANITA-IV was supported through NASA grant NNX15AC24G. Computing resources for this project were provided by the Research Computing Center at the University of Chicago and the UCLA Institute for Digital Research & Education. We gratefully acknowledge NSF CAREER awards 1752922 & 1255557, the CSU's Research, Scholarly, and Creative Activities Grant Program, the KAUST Gifted Student Program, the Cosmology and Astroparticle Student and Postdoc Exchange Network (CASPEN), the Leverhulme Trust, Taiwan's Ministry of Science and Technology (MOST) under its Vanguard Program 106-2119-M-002-011, and the Ministerio de Economía, Industria y Competitividad (FPA2017-85114-P and María de Maeztu Unit of Excellence MDM-2016-0692) and the Xunta de Galicia (ED431C 2017/07).

References

[1] ANITA, *Physical Review Letters* **117(7)**, 071101 (2016).

[2] ANITA, *Physical Review Letters* **121(16)** (2018).

[3] A. Romero-Wolf *et al.*, *Physical Review D* **99(6)** (2019).

[4] J. Alvarez-Muñiz *et al.*, *PRD* **97(2)**, 023021 (2018).

[5] A. Connolly, R. S. Thorne, and D. Waters, *Physical Review D* **83(11)**, 113009 (2011).

[6] H. Abramowicz and A. Levy, 1997, arXiv:hep-ph/9712415.

[7] N. Armesto, C. A. Salgado, and U. A. Wiedemann, *Physical Review Letters* **94(2)** (2005).

[8] M. Jezabek, Z. Was, S. Jadach, and J. H. Kuhn, *Comp. Phys. Comm.* **70(1)**, 69 (1992).

[9] T. Sjöstrand *et al.*, *Computer Physics Communications* **191**, 159 (2015).

[10] IceCube, *Physical Review Letters* **117(24)**, 241101 (2016).

[11] Auger, 2019, arXiv1906.07422.

[12] ANITA, *PRD* **98(2)**, 022001 (2018).

[13] IceCube, *Astrophysical Journal* **835 (2)**, 151 (2017).

[14] Auger, 2019, arXiv:1906.07419.